Paper: ASAT-15-120-CA

15th International Conference on
AEROSPACE SCIENCES & AVIATION TECHNOLOGY,
ASAT - 15 – May 28 - 30, 2013, Email: asat@mtc.edu.eg ,
Military Technical College, Kobry Elkobbah, Cairo, Egypt,
Tel: +(202) 24025292 –24036138, Fax: +(202) 22621908

Corrosion Behaviour of Novel AZ91-Ti Magnesium Titanium Matrix Composites in Dilute Harrison Solution

{M. Shamekh, M. Gobara[*]}[†]

Abstract: A novel magnesium magnesium alloy was prepared by adding titanium and barium carbide under argon environment. The mechanical properties of the prepared alloy were investigated with respect to the AZ91D alloy. The microstructure of the composites was investigated using Scanning Electron Microscope SEM/EDS and X-ray diffraction (XRD). The corrosion behaviour of magnesium matrix composites reinforced with a Titanium and boron network of particulates fabricated using a low cost in-situ reactive infiltration technique. The corrosion behaviour was examined using both AC and DC techniques; electrochemical impedance spectroscope (EIS) and potentiodynamic polarization in dilute Harrison solutions. The tafel extrapolation results showed that the corrosion rate reduce by an order of magnitude. Moreover; EIS results shows that addition of Ti and Barium carbide improve the corrosion behaviour of AZ91 alloy and no sign of corrosion was appeared during 10 days of immersion in corrosive environments.

Keywords: Corrosion TiC, TiB_2, AZ91D alloy and EIS

1. Introduction

Magnesium was discovered in 1774 and it is the sixth most abundant element in the Earth's crust (about 2%). Moreover, it is the third most abundant among the dissolved minerals in seawater [1].

Magnesium is the third most commonly used structural metal, following iron and aluminium. Magnesium and its alloys have a wide range of applications including automotive, aerospace, electronics, guided weapons industries and as alloying element in production of aluminium and steel [2]. Magnesium alloys have been used by designers due to their low density, strength to weight ratio, ease of machinability, high damping capacity, castability, weldability and recyclability. Magnesium is approximately two thirds the density of aluminium and a quarter that of steel [3]. However, magnesium has poor corrosion resistance, although, magnesium alloys form oxide layer on their surfaces, this layer non compact and leads to a poor corrosion resistance especially in chloride containing environments. The high corrosion rate is due to the high electron negative potential of Mg (-1.5V vs SCE) with respect to other materials such as zinc and aluminium (-1.0 and -0.8V respectively) which might lead to sever corrosion [4]. Moreover, impurities and second phases act as active cathodic sites that accelerate corrosion of the magnesium matrix [5, 6].

Due to rapid developing in magnesium industry and applications, engineers and designers are developing methods to improve the corrosion resistance of magnesium alloys by modifying alloy chemistry and improving surface protection technologies [3, 5]. In order to improve

[*] m_gobara@yahoo.com
[†] Egyptian Armed Forces, Egypt

magnesium mechanical properties and corrosion resistance, alloying elements are widely employed to improve microstructure [7]. Moreover, adding alloying elements such as Ca, Sb, Bi, Sn and Pb is an effective way to improve the mechanical properties of AZ91 alloys [8-14]. In our previous papers, Mg matrix composites reinforced with a network of TiC and TiB_2 particles have been successfully fabricated using a practical and low cost in-situ reactive infiltration technique. Also, the mechanical characterization of the fabricated composites was investigated and compared with the unreinforced AZ91D alloy matrix [15, 16].
The main objective of this work is to study the corrosion behavior of the fabricated composites showing the effect of the reinforcing phases and compared it with that of the commercial AZ91D alloy.

2. Experimental

2.1 Material

In this work, the material used is AZ91D magnesium matrix composites reinforced with a network of TiC- Ti_2AlC-TiB_2 particulates (TAZ composites) which were synthesized using a practical and low cost in-situ reactive infiltration technique. The in-situ reactive infiltration experiments were carried out in an electric furnace under the presence of flowing argon gas (purity ≥ 99.999%) as shown in
Fig. 1 (a). The molten Mg alloy infiltrates a preform of 75 wt.% ($3Ti_p$ + B_4C_p) +25 wt.% MgH_2 with 70% relative density (RD) at processing temperature of 900ºC for 1.5 h holding time. The samples were naturally cooled down to room temperature [15]. Details may be found elsewhere [15].
The microstructure and the phase analysis of the fabricated composite samples were investigated using scanning electron microscope (SEM) (Philips XL30 FEG) equipped with Energy Dispersive X-ray Spectroscopy (EDS) and X-Ray diffraction (XRD) using an (X'Pert PRO) X-ray diffractometer (PANalytical Inc.). It is important to note that Si is added to the powder sample during the XRD analysis as an internal standard to correct any systematic error.
The compression tests were performed on as-received AZ91D alloy and TAZ composites according to ASTM E9-89a [20]. Test specimens were machined to a round cross-section of 12.7 mm (1/2 inch.) in diameter and 25 mm (1 inch.) in height. Testing was performed on MTS 809 equipment, with a 250 kN load capacity at room temperature with a cross-head speed of 0.5 mm/min and no barreling was observed. Two strain gauges (CEA-06-125UW-350, Vishay Micro-Measurements) were installed longitudinally parallel to the load direction on the side of each test sample with 180º between them to measure the strain, as shown in
Fig. 1 (b) [16].
Magnesium alloy AZ91 samples (obtained as Q-panels) were cleaned with deionised water followed rinsing in acetone and then left to dry for 30 min at 60ºC, then cooled before corrosion testing at room temperature.
Corrosion tests were carried out in a three-electrode type cell using the sample (working electrode), a 'saturated' calomel reference electrode and a platinum counter electrode. Electrochemical impedance measurements are obtained at the measured E_{ocp} values applying ±10 mV perturbation, in the frequency range from $1x10^5$ Hz to 10^{-2} Hz. Electrochemical corrosion measurements were performed separately in dilute Harrison solution at room temperature and in open air with a Gamry reference 600 instrument with the solution being renewed every three days. The experimental results of the impedance were analyzed in terms of an equivalent circuit using Nonlinear
Least Squares Fit Technique provided by the Gamry software.

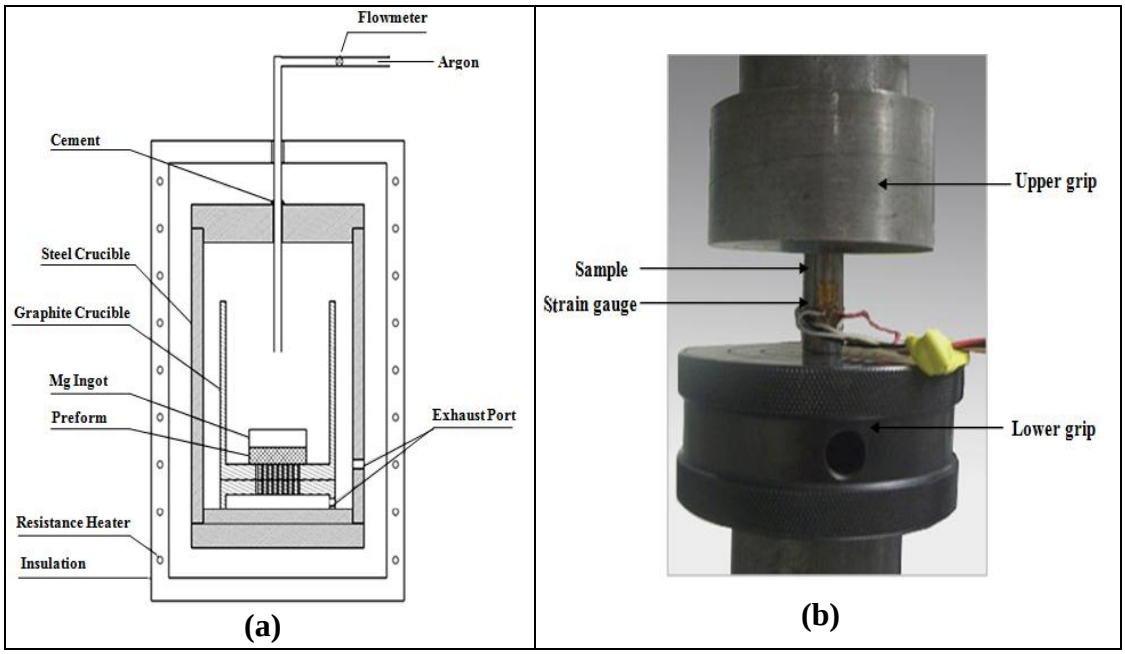

Fig. 1(a) Schematic experimental setup and (b) compression testing.

3. Results and Discussion

3.1 Mechanical Properties

The microstructure and the elemental mapping of the composite reveal a reasonably uniform distribution of reinforcing phases, as a network of TiC_x, Ti_2AlC and TiB_2 without any residual intermediate phases as shown in

Fig. 2. The elemental mapping reveals the existence of Al (AZ91 contains 9 wt% Al) not only inside the Mg matrix but also in the Mg-free regions proving the formation of the ternary compound (Ti_2AlC) [15].

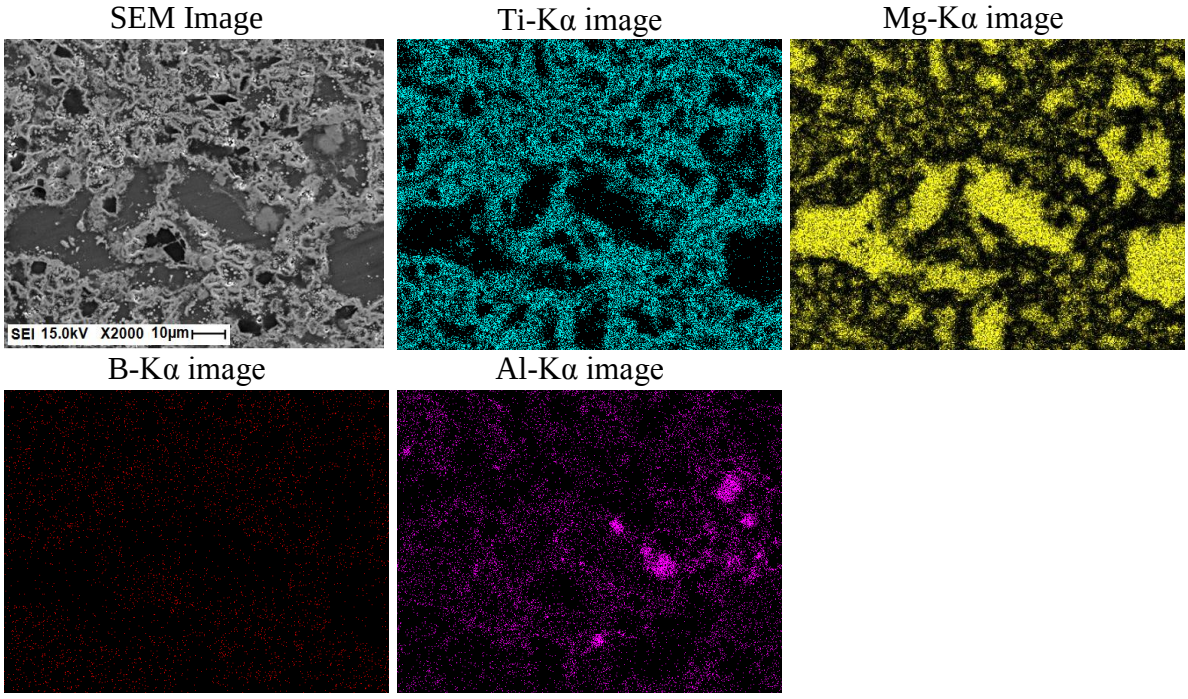

Fig. 2 SEM microstructure and EDS elemental mapping of the TAZ composites

As shown in Fig. 3, the XRD pattern of the composite samples reveals the complete formation of the reinforcing phases without residual intermediate phases. Ti_2AlC compound forms at the expense of TiC_x by the diffusion of Al from molten AZ91 alloy into the substoichiometric TiC_x at high temperature. Also, MgO was detected due to the decomposition of MgH_2 at low temperature forming Mg with high affinity to oxygen due, in part, to its high surface area [15].

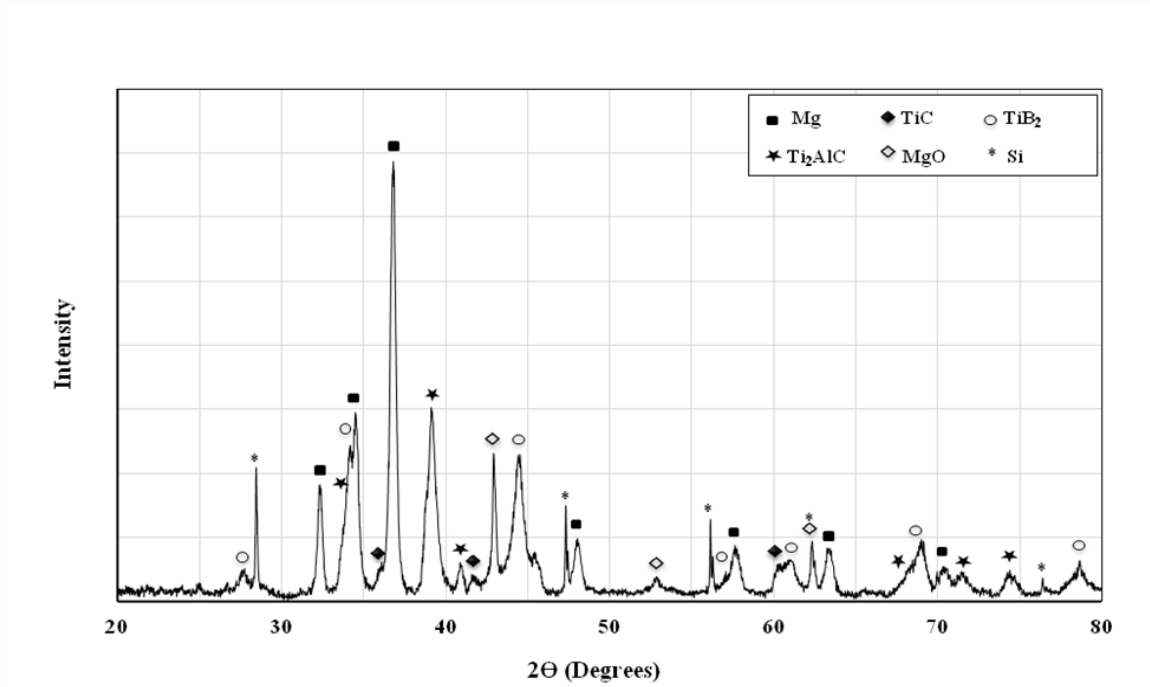

Fig. 3 XRD pattern of the TAZ composite

Typical compression behaviour of the TAZ composites compared with that of the unreinforced AZ91D alloy is given in Fig. 4. The results of the compression test revealed that the TAZ composites developed in this study exhibit higher modulus and compressive strength compared with those of the unreinforced AZ91D matrix while the ductility is reduced.

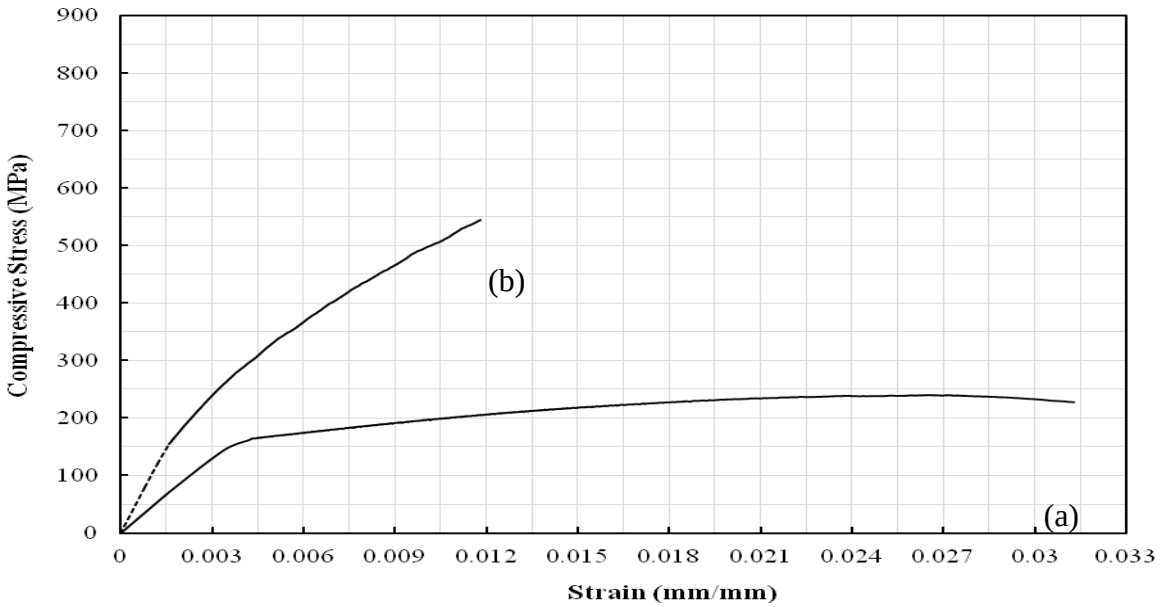

Fig. 4 Stress-strain curves of (a) the AZ91D alloy and (b) TAZ composite

The compression test results for these composites are summarized in Table 1. The compressive strength and Young's modulus of the composites increased by nearly 124% and 144%, respectively compared with those of the unreinforced AZ91D alloy while the ductility decreased by typically 62%. In general, the strength of the composite increased due to the formation of the reinforcing phases where the dispersion of fine and hard particles into the matrix blocks the dislocation motion and thus strengthens the material.

Table 1 Compression test results of the AZ91D alloy and TAZ composites.

Sample	Reinforcing phases (vol. %)	Young's Modulus, (GPa)	Compressive Strength (MPa)	Height reduction (%)
AZ91	-----	45	241	3.13
TAZ	~ 22	110 ±10.01	540 ±14.55	1.19 ±0.068

3.2 Corrosion Performance of the Alloys

Corrosion of multi-phase Mg alloy such as AZ91, in a corrosive solution like 3% NaCl, is governed by the composition of the alpha-Mg matrix, the composition and the distribution of the other phases. The alpha-Mg matrix has a corrosion rate significantly greater than that of beta phase in such corrosive solutions [17]. The second phase works as micro cathodes, with respect to alpha-Mg, forming micro localized galvanic cell that accelerating the corrosion rate of adjacent the alpha-Mg matrix by up to twenty fold [16].

3.2.1 Polarisation results

As a preliminary investigation the corrosion properties of AZ91 and TAZ was conducted using a polarisation technique in dilute Harrison solution. Anodic and cathodic branches were measured separately.

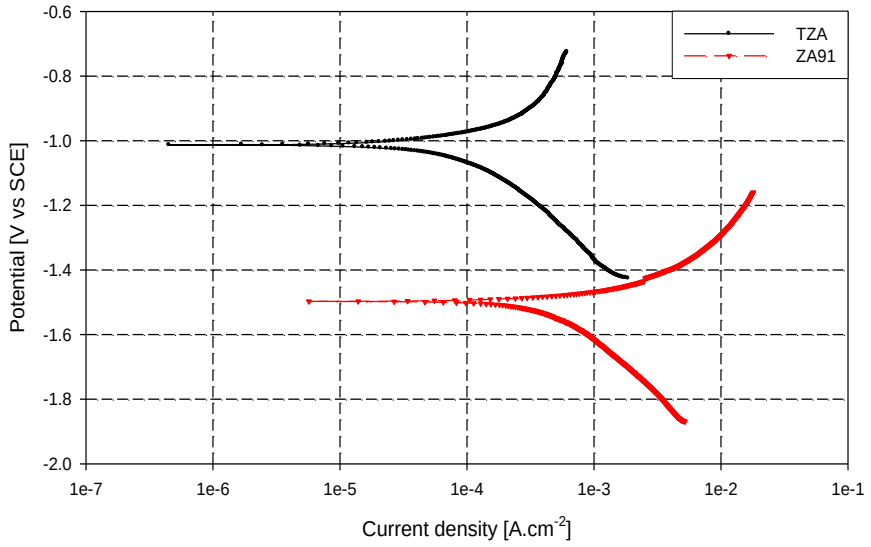

Fig. 5 Polarization curves for bare, AZ91 and TAZ in dilute Harrison solution

As shown from Fig. 5 the AZ91 sample has a corrosion current of about 3.56 mA/cm^2. The anodic branch of the AZ91 sample shows continuous active dissolution of the metal while the cathodic branch exhibits diffusion control (oxygen reduction reaction). In comparison, the corrosion current of the TAZ sample is one order of magnitude lower than that of AZ91

sample being 0.27mA/cm^2. The polarisation curve of TAZ sample, shown in Figure 1, exhibits a corrosion potential (1020V mV vs SCE) that is higher than that of AZ91 sample (1506V vs SCE). The polarisation data are summarised in following Table2.

Table 2 Polarization data

Sample	E_{corr} mV (vs SCE)	I_{corr} mA/cm^2
Bare AZ91	-1506±30	3.56
Bare TAZ	-1063±30	0.27

3.2.2 Electrochemical impedance results

Using Tafel extrapolation technique for measuring corrosion rate should take many concerns as the rate of magnesium alloys changes with the immersion time [17]. For comparison, EIS was used to evaluate the corrosion performance of both novel TAZ and AZ91alloy at an open-circuit potential after its immersion in freely aerated dilute Harrison solution.

Fig. 6 shows the impedance of the AZ91D in dilute Harrison solution. The figure shows that impedance at low frequency, is initially low (less than 10^2 Ohm.cm^2). However, with prolonged immersion, the impedance value increases by about one order of magnitude within 10 days.

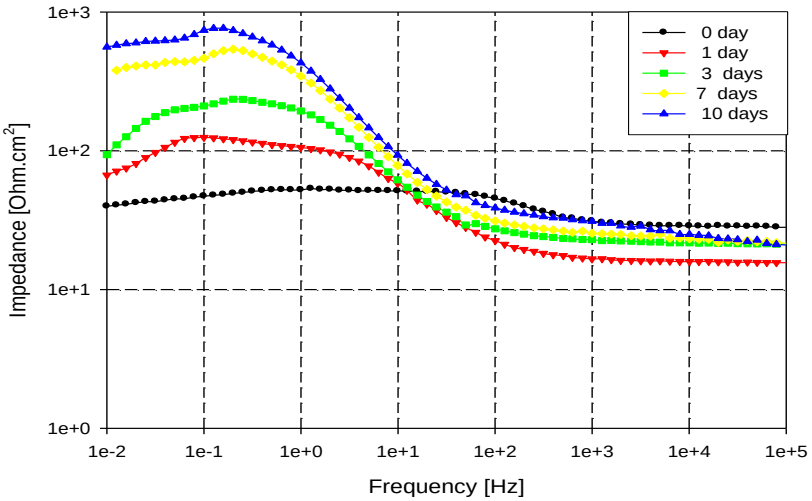

Fig. 6 Impedance behavior of bare AZ91 in dilute harrison solution

The phase angle curve, Fig. 6, showed two time constants; at 3x10^2 Hz and at 10 Hz after one hour of immersion. The former showed an increasing capacitive behaviour which may be related to the dissolution of magnesium leaving and formation of corrosion products, moreover, the surface' content of aluminium increased with time of immersion [18]. Furthermore, the magnitude of the time constant increased with time of immersion suggesting an increase in the corrosion resistance of the metal substrate as showed in Fig. 7. The latter time constant peak, at 10 Hz, may related to the reactivity of magnesium this peak disappeared after three days of immersion. Visual inspection reveals that a vigorous reaction of magnesium takes place directly after immersion in Harrison solution which is related to the reduction of hydrogen on the magnesium surface. This reaction disappeared after two days of immersion.

This behaviour was accompanied by the appearance of gelatinous insoluble precipitate on the surface of AZ91 sample after 3 days of immersion in the electrolyte which may relate to the formation of magnesium hydroxide [19].

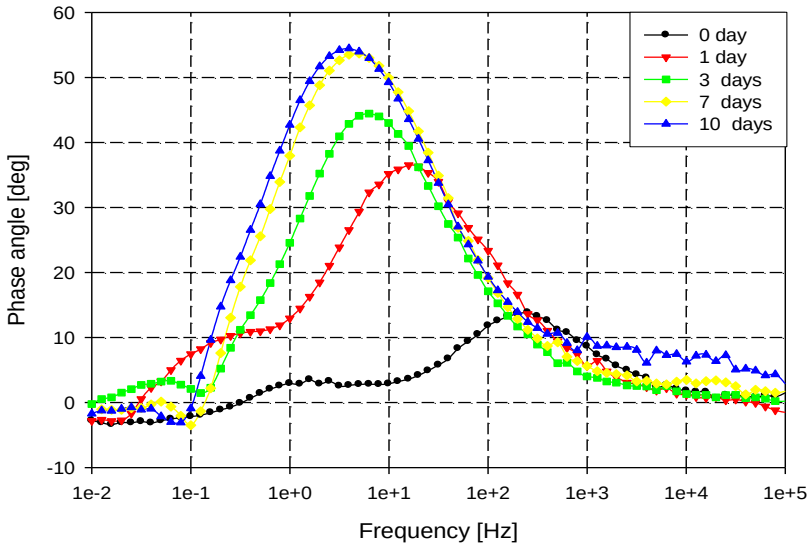

Fig. 7 Phase angle response of bare AZ91 in dilute Harrison solution.

The SEM image of AZ91 after 10 days of immersion in dilute Harrison solution is showed in Fig. 8. The image reveals a localised corrosion around β-phase interfaces, forming a micro-galvanic cell with the surrounding Mg matrix [18]. Examination of the surface revealed heavy corrosion over the entire metal surface (
Fig. 8-b) with individual shallow pitting being observed due to that β-phase particles leave the surface producing a vacant sits (arrows in **Error! Reference source not found.**-a).

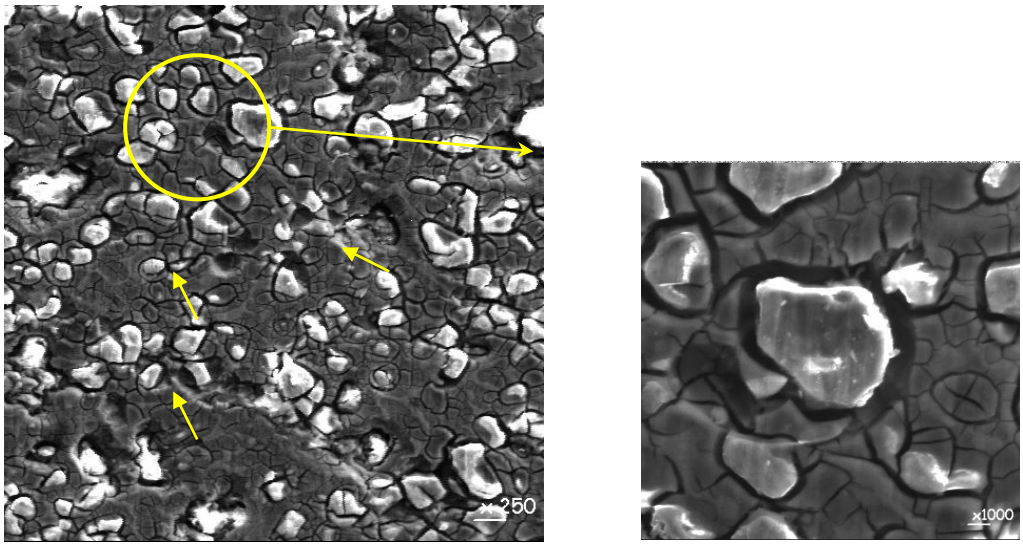

Fig. 8 SEM image of bare AZ91 sample after immersion for 10 days in dilute Harrison solution.

Bode and phase angle plots for TAZ in dilute Harrison solution are shown in Fig. 9 and Fig. 10 respectively. As seen from **Error! Reference source not found.**, the impedance shows an inductive peak in the impedance curve was observed after one hrs of immersion; however, this completely disappeared before the 3 days measurement due to induced metastable Mg^{+} ions in series with a charge transfer resistance [20].

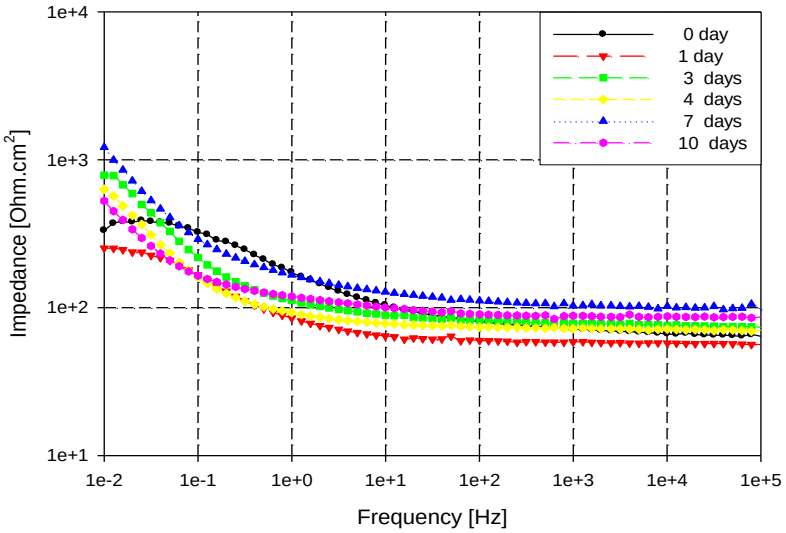

Fig. 9 Impedance behavior of bare TAZ in dilute Harrison solution

Fig. 9, the impedance behaviour of TAZ sample, shows a small change in low frequency impedance during 10 of immersion in dilute Harrison solution, notably a small increase in the impedance after one day of immersion. After 3 days of immersion, the impedance became stable. The phase angle curve, **Error! Reference source not found.**, shows that there are two time constants at about $5x10^{4}$ and 1.0 Hz. The former displays a slightly decrease with immersion time, however, the latter increased by prolonged immersion, whilst at the same time, moving towards low frequency region. Physical observation of the TAZ sample shows a strong reaction takes place directly after immersion in Harrison solution which is related to the reduction of hydrogen on the magnesium surface. This reaction disappeared after two days of immersion and neither sign of corrosion or precipitation on the metal surface was observed.

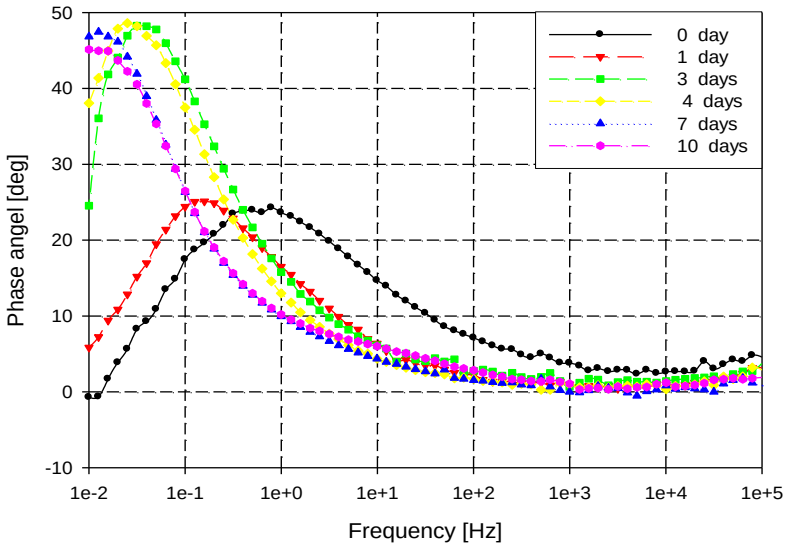

Fig. 10 Phase angle response of bare TAZ in dilute Harrison solution

The Nyquist plots of the TAZ sample in dilute Harrison solution, Fig. 11, shown that there is an inductive loop appeared before 24 hr of immersion in the low frequency range, however, this loop disappeared after that. The aforementioned loop usually emerges with the dissolution of metal [21, 22]. It is believed that the inductive loop in the low frequency range of magnesium alloys reflects dissolution of magnesium protective layer. Therefore, disappearing of the inductive loop indicated that a more perfect protective film is formed on the magnesium surface [23].
also agree with this point.Moreover, the figure showed that there is a capacitive behaviour begin after 24hr and increases with immersion time.

The EIS spectra were analysed by fitting to the equivalent circuit model shown in Fig. 12.

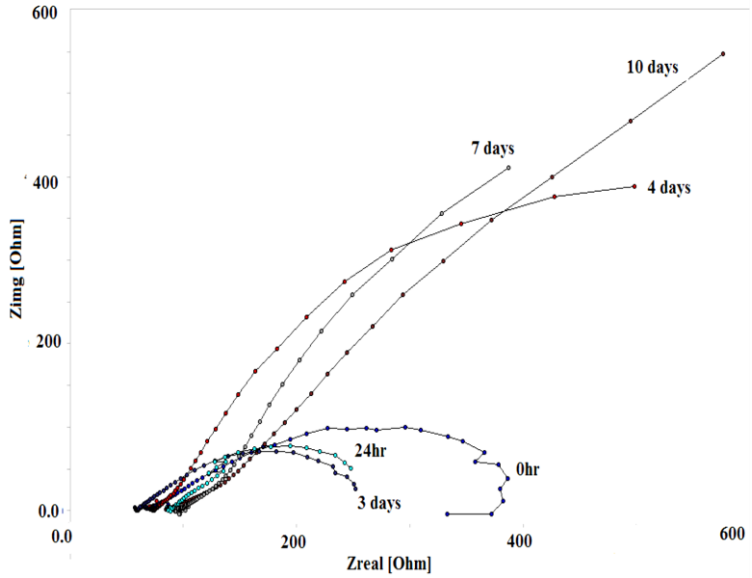

Fig. 11 Nyquist plots of bare TAZ in dilute Harrison solution

The parameters obtained by fitting the equivalent circuit in addition to the Goodness of Fit are listed in Table 3. In Fig. 12 (a), R_u represents the solution resistance between the alloy and the counter (platinum) electrode, C the double layer capacitance, R_p is the double layer resistance and the L is is an inductive loop related to instability due to dissolution of the outer layer of the TAZ alloy. However, in Fig. 12 (b) R_u represents the solution resistance between the alloy and the counter (platinum) electrode,$Ø_7$ and $Ø_5$ are the constant phase elements (CPEs) for the double layer and formed layer on the Mg alloy surface.
The value of goodness of fitting (less than $3x10^{-3}$) indicates that the proposed simulated circuits, Fig. 12, properly fitted.

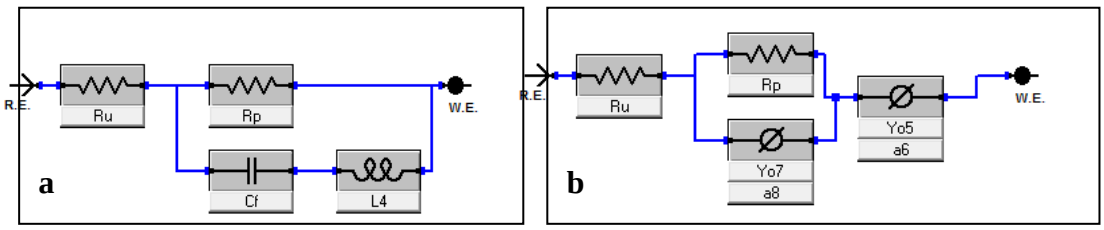

Fig. 12 Equivalent circuits model used to fit the EIS experimental data a) before 24hrs, b) after 24 hrs of immersion in dilute Harrison solution

Table 3 Electrochemical parameters from EIS in dilute Harrison solution

	0 hr	24 hr	3 days	4 days	7 days	10 days
R_p	243.4	199.5	644.8	675.3	680	600
R_u	74.04	54.33	74.47	70.5	94.71	84.37
C	1.11E-03					
$Ø_7$		0.06994	0.01321	0.02136	0.01714	0.0159
a_7		0.1563	0.3787	0.3843	0.3864	0.317
$Ø_5$		0.008896	0.0169	0.023	0.04168	0.041
a_5		0.7284	1	0.9632	1	1
L	4.40E-03					
Goodness of Fit	0.003	0.002	0.003	0.0003	0.0009	0.00047

The value of CPE of the producing layer on the magnesium surface with immersion time is shown in Fig. 13. The figure showed that the value of CPE increased with immersion time then become stable after 7 days if immersion. Moreover, the value of a_5 is almost 1 which indicates that the CPE have a capacitance behavior.

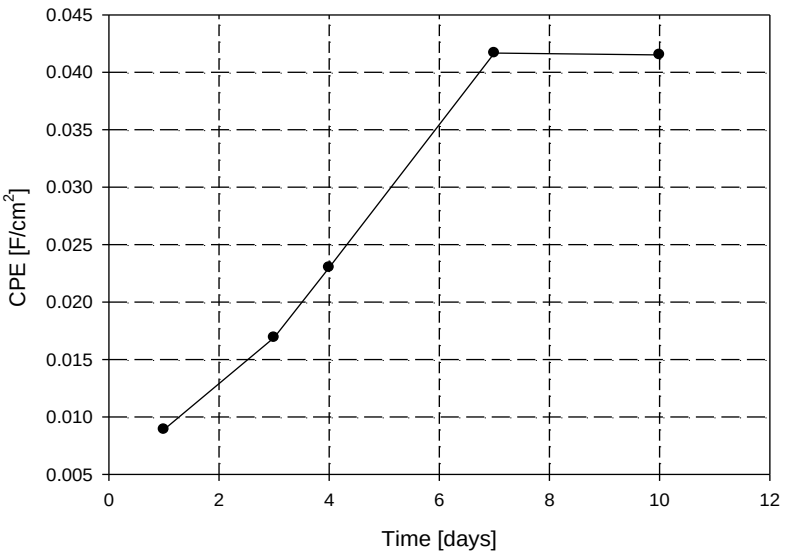

Fig. 13 CPE with time of immersion in dilute Harrison solution

This behaviour of increasing in the CPE of the formed layer was accompanied with distinguished increase in the corrosion potential as shown in Fig. 14.
The SEM of TAZ sample,
Fig. 15, showed that the surface of the sample became rough, with respect to the original surface
Fig. 2; moreover, the alpha-Mg pond showed in
Fig. 2 disappeared.
From the above discussion, it could be concluded that the improve in corrosion performance of TAZ (with respect to AZ91D) refers to the disillusion of alpha-Mg from the TAZ surface during first few hours of immersion in the corrosive solution leaving titanium carbide and boride phases which has better corrosion performance than that of alpha magnesium. That can be confirmed by the increase of corrosion potential of TAZ with immersion time.

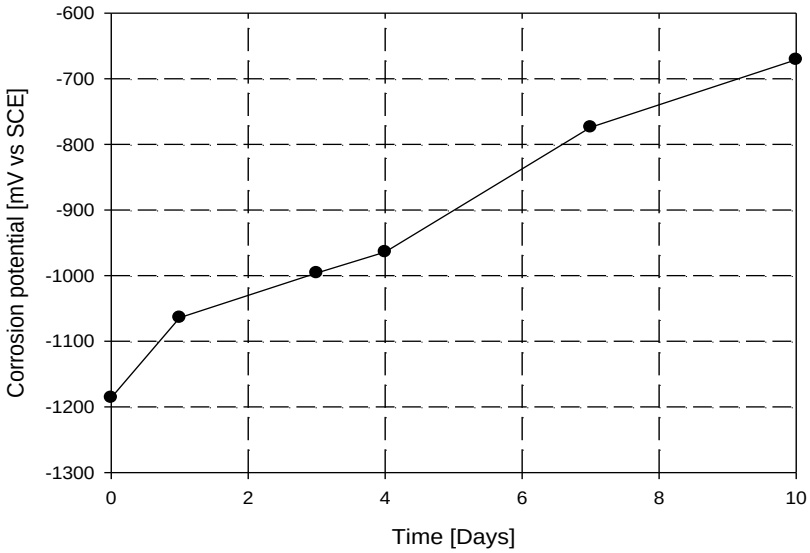

Fig. 14 Changing of Corrosion potential of TAZ sample with immersion time in dilute Harrison solution

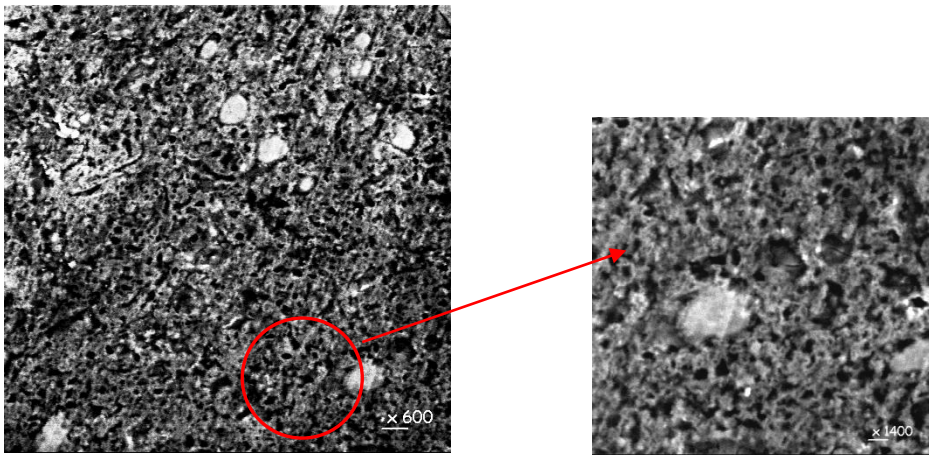

Fig. 15 SEM image of bare TAZ sample after immersion for 10 days in dilute Harrison solution.

4. Conclusions

1) The results of the mechanical characterization revealed that TAZ exhibit enhanced mechanical properties compared with the commercial AZ91D alloy.
2) The corrosion performance of the AZ91D alloy is improved by adding ceramic particles such as titanium carbide and titanium boron.
3) The novel TAZ alloy exhibit better corrosion performance than commercial AZ91 alloy by removing the alpha magnesium phase from the outer surface of the novel alloy.

References

[1] K.U. Kainer, in Magnesium-Alloys and Technology, Wiley-VCH Verlag GmbH & Co, Weinheim, Germany, 2003, pp. 1–22.

[2] Edward Ghali, Corrosion Resistance of Aluminium and magnesium Alloys, John Wiley & Sons, Inc., New York, 2010, p. 321.

[3] E. Ghali, Magnesium and magnesium alloys, in: R.W. Revie (Ed.), Uhlig's Corrosion Handbook, John Wiley & Sons, New York, 2000, p. 793.

[4] Heming Wang, Mohamed Gobara, Robert Akid, 8th international conference of Magnesium alloyed and its applications, 2009.

[5] G.L. Song, A. Atrens, Advanced Engineering Materials, 2003, 5, 837.

[6] El-Sayed M. Sherif , Abdulhakim A. Almajid , Int. J. Electrochem. Sci., 2011, 6, 2131 – 2148

[7] S. Candana, M. Unalb, E. Kocb, Y. Turenb, E. Candana,, Journal of Alloys and Compounds, 2011, 509, 1958–1963

[8] D. Wenwen, S. Yangshan, M. Xuegang, X. Feng, Z. Min, W. Dengyun, Mater. Sci. Eng,. 2003, A 356, 1–7.

[9] G. Wu, Y. Fan, H. Gao, C. Zhai, Y.P. Zhu, Mater. Sci. Eng., 2005, A 408, 255–263.

[10] W. Zhou, N.N. Aung, Y. Sun, Corros. Sci., 2009, 51, 403–408.

[11] Y. Guangyin, S. Yangshan, D. Wenjiang, Mater. Sci. Eng., 2001, A 308, 38–44.

[12] F. Wang, Y. Wang, P. Mao, B. Lu, Q. Guo, Trans. Nonferrous Met. Soc., 2010, 20, 311–317.

[13] Y. Guangyin, S. Yangshan, D. Wenjiang, Scr. Mater., 2000, 43, 1009–1013.

[14] B.H. Kim, S.W. Lee, Y.H. Park, I.M. Park, J. Alloys Compd., 2010, 493, 502–506.

[15] M. Shamekh, M. Pugh, M. Medraj, J. of Materials Chemistry and Physics, 2012, 135, 193-205.

[16] M. Shamekh, M. Pugh, M. Medraj, Advanced engineering materials, Vol. 135 (2012), 193-205.

[17] ASTM E9-89a, , American Society for Testing and Materials, 1989.

[18] A. Pardo, M. C. M., A.E. Coy, R. Arrabal, F. Viejo, E. Matykina, Corrosion Science 2008, 50, (3), 823 - 834.

[19] Patnaik, P., Handbook of Inorganic Chemicals. McGraw-Hill Companies: New York, USA, 2003.

[20] Jian Chen, J. W., Enhou Han, Junhua Dong, Wei Ke, Electrochimica Acta 2007, 52, (9), 3299 - 3309.

[21] Y. Xin, C. Liu, W. Zhang, J. Jiang, G. Tang, X. Tian, and P. Chu, Journal of The Electrochemical Society, 155, 5, C178-C182, 2008.

[22] Lingjie Li, Fusheng Pan and Jinglei Lei (2011). Environmental Friendly Corrosion Inhibitors for Magnesium Alloys, Magnesium Alloys - Corrosion and Surface Treatments, Frank Czerwinski (Ed.), Available from: http://www.intechopen.com/books/magnesium-alloys-corrosion-and-surface-treatments/environmental-friendly-corrosion-inhibitors-for-magnesium-alloys

[23] T. Zhang, C. Chena, Y. Shao, G. Meng, F. Wang, X. Li, C. Dongc, Electrochimica Acta, 53 (2008) 7921–7931